

A Fresh Look at the Role of the Coupling of a Discrete state with a Pseudo-continuum State in the Stabilization Method for Characterizing Metastable States

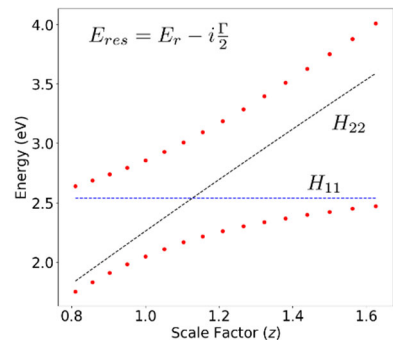
Benjamin J. Carlson¹, Michael F. Falsetta¹, Stephen R. Slimak², and Kenneth D. Jordan^{2*}

¹ Department of Chemistry, Grove City College, Grove City, Pennsylvania 16127 United States

² Department of Chemistry, University of Pittsburgh, Pittsburgh, PA 15260, United States

ABSTRACT: The stabilization method is widely used to theoretically characterize temporary anions and other systems displaying resonances. In this approach information about a metastable state is encoded in the interaction of a diabatic discrete state and discretized continuum solutions, the energy of which are varied by scaling the extent of the basis set. In this work, we identify the aspects of the coupling between the discrete state and the discretized continuum states that encode information about the existence of complex stationary points, and, hence, complex resonance energies in stabilization graphs. This allows us to design a simple two-level model for extracting complex resonance energies from stabilization graphs. The resulting model is applied to the ${}^2\Pi_g$ anion state of N₂.

TOC Graphic



Keywords: stabilization method, temporary anion, scattering resonance, analytic continuation

Anion states that lie energetically above the electronic ground state of the neutral atom or molecule are metastable as they are subject to electron detachment. Temporary anion (TA) states are important in several fundamental and applied areas and appear as resonances in various electron scattering cross sections.¹⁻³ TAs often have lifetimes on the order of 10-100 femtoseconds, similar to the timescale for molecular vibration. In the Siegert picture,⁴ a temporary anion is characterized by a complex energy, $E_{res} = E_r - i \Gamma/2$, where E_r and Γ give the resonance position and width, respectively (here atomic units are employed). Γ^{-1} thus corresponds to the anion lifetime. Modelling cross sections from electron-molecule scattering experiments requires accurate determination of both the energy of the anion state relative to the neutral and the anion lifetime as a function of molecular geometry.

Straightforward application of standard quantum chemistry methods to TAs is not possible when using flexible basis sets needed for accurate results due to the presence of discretized continuum (DC) solutions that fall energetically below and in the same energy range as the temporary anion of interest. The DC solutions correspond to a free electron as described by the finite basis set. Several methods have been introduced for the calculation of complex energies associated with resonances.⁵⁻¹¹ One of the simplest, in the sense that it can be used with electronic structure codes without modification, is the stabilization method⁵ in which one calculates the energies of multiple eigenvalues of the appropriate symmetry of the excess electron system as a function of a scale parameter, z , that controls the spatial extent of the basis set. A plot of the eigenvalues vs z displays avoided crossings that can be interpreted as resulting from the mixing of a relatively compact diabatic discrete state, the energy of which is independent or only weakly dependent on the scale parameter, and DC solutions whose energies

depend strongly on the scale parameter. A stabilization graph for the widely studied $^2\Pi_g$ anion state of $\text{N}_2^{1,11-14}$ at the equilibrium geometry of the neutral molecule is displayed in Figure 1. The results reported in Figure 1 were generated using the electron affinity equation of motion Møller-Plesset (EA-EOM-MP2)^{19,20} method, scaling by a factor of z the exponents of four diffuse p functions in a modified aug-cc-pVTZ Gaussian-type orbital (GTO) basis set^{21,22} described in Reference 14. The energies are reported relative to that of the neutral molecule. The calculations were carried out using the CFOUR code.²³

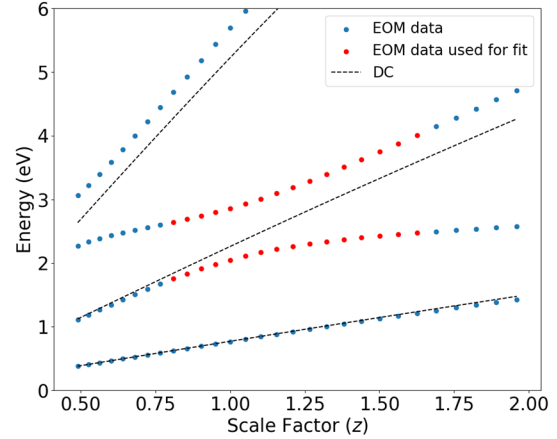


Figure 1. Stabilization graph for the $^2\Pi_g$ anion of N_2 . The dashed lines give the energies of the DC levels and the dots the energies of the excess electron levels from the EOM calculations.

Figure 1 also reports as a function of z the energies of the three lowest DC levels obtained from the one-electron Hamiltonian neglecting interactions with the nuclei and employing the same basis set as used in the EOM calculations. It is seen that the EOM calculations give one more energy level in the energy range displayed than there are DC levels. This extra level is due to the presence of the temporary anion state. The avoided crossing between the second and third eigenvalues near $z = 1$ can be viewed as occurring between the discrete state and the second DC level.

A variety of methods have been introduced to extract resonance parameters from stabilization graphs.¹⁵⁻¹⁸ In the case of relatively sparse stabilization graphs, determination of the

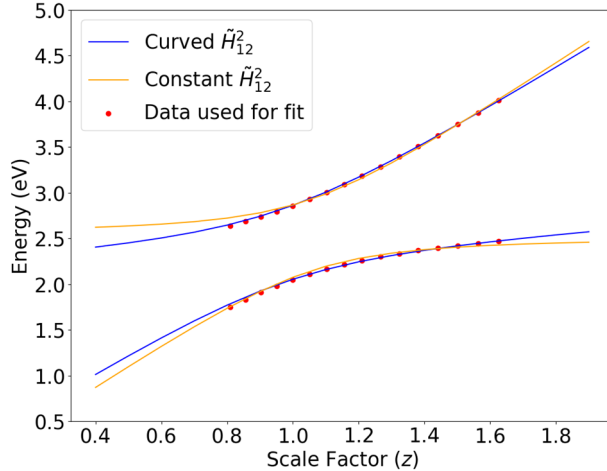


Figure 2. Eigenvalues (in eV) *vs* z of two model Hamiltonians derived from the stabilization graph shown in Figure 1. Results obtained with \tilde{H}_{12}^2 including a term quadratic in z are shown as blue lines and those with a constant \tilde{H}_{12} are shown as orange lines. The ab initio input data are shown as red dots.

method have long been appreciated, the fundamental physical requirements for the presence of complex stationary points from stabilization graphs are not fully understood. That this is a subtle issue is illustrated in Figure 2 which reports the eigenvalues of two model 2x2 Hamiltonians that approximately reproduce the avoided crossing near $z = 1.0$ in the stabilization graph for N_2^- reported in Figure 1. Even though the curves from the two models are similar, a complex stationary point that gives realistic resonance parameters is found for only one of the two models. This leads naturally to the question of what aspects of the Hamiltonian matrix elements are responsible for the existence of complex stationary points associated with the analytically continued eigenvalues of a stabilization calculation, and this is the primary focus of this study.

In order to analytically continue the energies from stabilization calculations into the complex plane, one assumes a functional form for E in terms of z and fits the data points on the

complex resonance energy can be accomplished by analytically continuing the energies as a function of z into the complex plane and locating complex stationary points at which $\frac{dE}{dz} = 0$. Substitution of the appropriate stationary point into the expression for E gives the complex resonance energy.¹⁷ While the intuitive appeal and ease of implementation of the stabilization

stabilization graph to determine the parameters in this function. While one can employ data remote from the avoided crossing using Padé approximants²⁴ for the analytic continuation, in our applications we have focused on data points near an avoided crossing and have used generalized Padé approximants (GPAs),²⁵ which build in the branch point structure. In the present study we find it useful to view a region of a stabilization graph displaying a reasonably well isolated avoided crossing as arising from a 2x2 eigenvalue problem involving a diabatic discrete state with energy H_{11} and a single diabatic DC level with energy H_{22} and their coupling, H_{12} . The diabatic states are not orthogonal, and it is important to explicitly consider the effects of orthogonalization. We designate the wave functions corresponding to the discrete state and the DC level by ψ_1 and ψ_2 , respectively. We then orthogonalize ψ_2 to ψ_1 giving $\tilde{\psi}_2$. Allowing for the orthogonalization, the relevant matrix elements are

$$\tilde{H}_{22} = \frac{H_{22} - 2SH_{12} + S^2H_{11}}{1 - S^2} \quad (1)$$

$$\tilde{H}_{12} = \frac{H_{12} - SH_{11}}{\sqrt{1 - S^2}} \quad (2)$$

where $S = \langle \psi_1 | \psi_2 \rangle$ is the overlap of the two diabatic states, and the tilde indicates that overlap has been included in evaluating the matrix elements.

The resulting adiabatic levels, E_+ and E_- , are given by

$$E_{\pm} = \frac{H_{11} + \tilde{H}_{22}}{2} \pm \frac{1}{2} \sqrt{(H_{11} - \tilde{H}_{22})^2 + 4\tilde{H}_{12}^2} \quad (3)$$

The sum of the two eigenvalues is

$$E_+ + E_- = H_{11} + \tilde{H}_{22} \quad (4)$$

and their difference squared is

$$(E_+ - E_-)^2 = (H_{11} + \tilde{H}_{22})^2 + 4(\tilde{H}_{12}^2 - H_{11}\tilde{H}_{22}) \quad (5)$$

Thus, one can directly extract $H_{11} + \tilde{H}_{22}$ and $(\tilde{H}_{12}^2 - H_{11}\tilde{H}_{22})$ from the adiabatic curves of a stabilization graph provided it has a region with an isolated, well-defined avoided crossing.

Both $H_{11} + \tilde{H}_{22}$ and $\tilde{H}_{12}^2 - H_{11}\tilde{H}_{22}$ are found to display a near linear dependence on z , however as

seen from Figure 2, small deviations from

linearity of the latter quantity can prove

essential to the existence of complex

stationary points. It is important to note that

this nonlinearity can result from \tilde{H}_{12}^2 or H_{11}

\tilde{H}_{22} or from both terms. With the assumption

that H_{11} is independent of z , one can extract

\tilde{H}_{22} from the stabilization graph by use of Eq. (4). A constant H_{11} can be accomplished by designing the basis set so that in the absence of the functions that are scaled its energy is close to the experimental electron attachment energy. More formally this can be accomplished by use of

Feshbach projection operators.²⁶ With the assumption that H_{11} is constant and using the \tilde{H}_{22}

curve deduced from the stabilization graph, one can obtain \tilde{H}_{12}^2 from Equations 4 and 5. Figure

3 displays the \tilde{H}_{12}^2 curve derived in this manner from the stabilization graph of N_2^- , using a H_{11}

value of 2.44 eV, obtained by fitting to the model described below. The resulting curve has a

maximum near $z = 1.00$, which is close to the crossing point of the orthogonal diabatic curves.

Calculations using model potentials indicate that H_{12} varies monotonically with z and is

dominated by the kinetic energy contribution and that the existence of a maximum in \tilde{H}_{12}^2 is a

consequence of the presence of the overlap contribution in Eq. 2.²⁷ We demonstrate below that

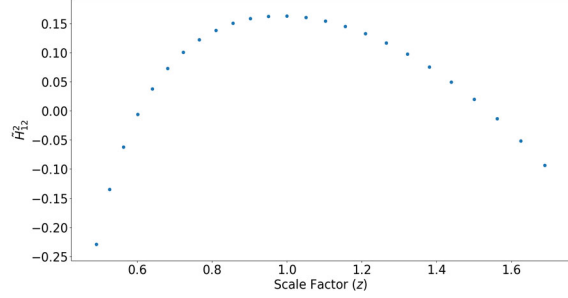


Figure 3. \tilde{H}_{12}^2 vs. z extracted from the EOM-MP2 stabilization graph for N_2^- . Results obtained with $H_{11} = 2.44$ eV.

the negative curvature in \tilde{H}_{12}^2 is essential for the existence of the complex stationary point corresponding to the resonance when H_{11} is taken to be constant.

The \tilde{H}_{12}^2 curve shown in Figure 3 is negative for z values less than about 0.6 and greater than about 1.5. The explanation for this seemingly unphysical behavior is straightforward: the stabilization graph shown in Figure 1 displays evidence that E_- is destabilized at larger z values considered by the lower lying DC level and that E_+ is stabilized at smaller z values by interaction with a higher lying DC level. The interaction with these other levels causes the \tilde{H}_{12}^2 curve extracted as described above to become negative and reflects a breakdown of the two-level model. However, it should be noted that the resonance parameters obtained using data for which negative values of \tilde{H}_{12}^2 are excluded from the fitting are essentially the same as when such data points are included. We have also considered a two-level treatment - one basis function for the discrete state and one for the DC level - for a square well plus rectangular barrier model potential and found for that case that the extracted \tilde{H}_{12}^2 is positive for all values of the scale parameter.

Based on the results presented above we introduce a simple, physically motivated model for extracting resonance parameters from a stabilization graph. The matrix elements in this model are:

$$H_{11} = a_0 \quad (6)$$

$$\tilde{H}_{22} = a_0 + a_1(z - z_1), \quad (7)$$

and

$$\tilde{H}_{12}^2 = A + B(z - z_1)^2 \quad (8)$$

where a_0 , a_1 , A , B , and z_1 are free parameters.

Note that with H_{11} taken as constant, extending the definition of \tilde{H}_{22} to include non-linear terms leads to cubic and higher order terms in $z-z_1$ in the square root in Equation 3. For characterizing the stationary points, these are less important than the quadratic term introduced via Equation 8. Hence, for this model curvature in \tilde{H}_{12} ² is more important than that in \tilde{H}_{22} .

The curves depicted in Figure 2 for which there are complex stationary points were derived by fitting the model Hamiltonian described above to the data indicated in red in the stabilization graph for N_2^- shown in Figure 1. The orange curves in Figure 2 that do not lead to complex stationary points were derived from the same model but retaining only the constant term in the coupling.

The complex resonance energy resulting from the quadratic model given by Equations 6 through 8 is $2.44 - 0.29i$ eV, in good agreement with $2.53 - 0.24i$ eV result from a high-order GPA and with other values from the literature.^{1,11-14} We also extended the representation of \tilde{H}_{12} ² to include a cubic term, but this extension had negligible impact on the resonance parameters determined from the stabilization graph in Figure 1.

The quadratic model yields simple analytical expressions for the stationary points and resonance parameters. The relevant stationary point is

$$z^* = z_1 - \sqrt{\frac{a_1 A}{|B|(a_1^2 + 4B)}} i \quad (9)$$

where B is negative and a_1^2 is greater than $4B$ in magnitude. Note that since A and a_1 are necessarily positive, the existence of the complex stationary point is due to B being negative. The corresponding resonance energy is

$$E_{res} = a_0 - 2i \left[\left(\frac{\sqrt{A|B|}}{\sqrt{4B + a_1^2}} \right) \right] \quad (10)$$

With the assumption that a_1^2 is much greater than $4B$ in magnitude, the half width reduces to $2\sqrt{A|B|}/a_1$. For the stabilization graph of N_2^- shown in Figure 1, $a_1 = 2.54$ eV, and A and $B = 0.16$ and -0.55 eV², respectively. The half width obtained from $2\sqrt{A|B|}/a_1$ is 0.25 eV, compared to 0.29 eV from Equation 10. Interestingly, the expression for the resonance energy given by Equation 10, is independent of z_1 . At least in the case of the stabilization graph considered for N_2^- , nearly the same resonance parameters are obtained if z_1 is constrained to equal $z_0 = a_0/a_1$ which corresponds to the point at which the diabatic curves cross. Indeed, the optimized z_1 is found to be close to z_0 , and the reason that the resonance parameters change slightly when this constraint is imposed is that it introduces small changes in the other parameters, i.e., a_1 , A , and B .

Simons has also introduced a simple model for extracting resonance parameters from stabilization graphs.¹⁵ In the Simons model H_{11} and H_{22} are defined as $c_0 + c_1z$ and $d_0 + d_1z$, respectively, and with the coupling between the discrete state and the DC level being taken to be constant (V_0). Although the Simons model appears to be fundamentally different from that presented here, in both it and our model the complex stationary points derive from the presence of the quadratic z dependence in the $\tilde{H}_{12}^2 - H_{11}\tilde{H}_{22}$ term in the square root of a two-level model: in the Simons model this dependence enters via the $H_{11}\tilde{H}_{22}$ term and in our model it enters via \tilde{H}_{12} . Moreover, the two models can be related by a rotation of the basis functions representing the discrete and DC levels involved in the avoided crossing. We have confirmed that our model based on Equations 6-8 and Simons' model give identical resonance parameters

when fit to the data in the stabilization graph. (A fit of the Simons model to our stabilization data for N₂ gives $c_0 = 2.102$, $c_1 = 0.241$, $d_0 = 0.159$, $d_1 = 2.302$, and $V_0 = 0.304$ with energies in eV.)

Nonetheless, we believe that our model has the advantages of being consistent with a Feshbach operator approach (where H_{11} is constant) and making explicit the role that overlap between the discrete state and the DC level involved in an avoided crossing of the stabilization graph.

In summary, we have presented a two-level analysis of stabilization graphs for characterizing metastable states in which the negative curvature in the off-diagonal coupling between a diabatic discrete state and a diabatic discretized continuum state is shown to be essential for the encoding of information about the resonance in the stabilization graph. This curvature is a consequence of the overlap between the two diabatic states. In addition, based on this analysis we introduced a simple model for extracting the resonance parameters from the region of an avoided crossing.

Acknowledgements: This research was supported by a grant from the National Science Foundation under grant CHE1762337. MFF and BJC acknowledge support from the Swezey research fund at Grove City College. We thank K. Gasperich, J. Simons, and T. Sommerfeld for valuable discussions.

References

1. Schulz, G. Resonances in Electron Impact on Diatomic Molecules. *Rev. Mod. Phys.* **1973**, *45*, 423-486.
2. Allan, M. Measurement of Absolute Cross Sections of Electron Scattering by Isolated Molecules, in: *Low-Energy Electron Scattering from Molecules, Biomolecules and Surfaces*, *P. Carsky and R. Curik, eds.*, CRC Press **2012**, 43-90.
3. Jordan, K. D.; Burrow, P. D. Temporary Anion States of Polyatomic Hydrocarbons, *Chem. Rev.* **1987**, *87*, 557-588.
4. Siegert, A. J. On the Derivation of the Dispersion Formula for Nuclear Reactions. *Phys. Rev.* **1939**, *56*, 750-752.
5. Hazi, A. U.; Taylor, H. S. Stabilization Method of Calculating Resonance Energies: Model Problem. *Phys. Rev. A* **1970**, *1*, 1109-1120.
6. Aguilar S.; Combes J. M. *Commun. Math. Phys.* **1971**, *22*, 265.
7. Balslev E.; Combes J. M. *Commun. Math. Phys.* **1971**, *22*, 280.
8. Simon, B. *Int. J. Quantum Chem.* **1978**, *14* 529.
9. Riss, U. V.; Meyer, H.-D. Calculation of Resonance Energies and Widths Using the Complex Absorbing Potential Method. *J. Phys. B* **1993**, *26*, 4503-4535.
10. McCurdy, C. W. Jr.; Rescigno, T. N. Extension of the Method of Complex Basis Functions to Molecular Resonances. *Phys. Rev. Lett.* **1978**, *41*, 1364.
11. Jagau, T.-C.; Bravaya, K. B.; Krylov, A. I. Extending Quantum Chemistry of Bound States to Electronic Resonances. *Annual Rev. of Phys. Chem.*, **2017**, *68*, 525-553.

12. Chao, J. S. Y.; Falcetta M. F.; Jordan, K. D. Application of the Stabilization Method to the N_2^- ($\text{X}^2\Pi_g$) and Mg^- (1^2P) Temporary Anion States. *J. Chem. Phys.* **1990**, *93*, 1125-1135.

13. Dube, L.; Herzenberg, Absolute Cross Sections from the Boomerang Model for Resonant Electron-Molecule Scattering, *A. Phys. Rev. A* **1979**, *20*, 194-213.

14. Falcetta, M. F.; DiFalco, L. A.; Ackerman, D. S.; Barlow, J. C.; Jordan, K. D. "Assessment of Various Electronic Structure Methods for Characterizing Temporary Anion States: Application to the Ground State Anions of N_2 , C_2H_2 , C_2H_4 and C_6H_6 ", *J. Phys. Chem. A* **2014**, *118*, 7489–7497.

15. Simons, J. Resonance State Lifetimes from Stabilization Graphs. *J. Chem. Phys.* **1981**, *75*, 2465.

16. Isaacson A. D.; Truhlar, D. G. Single-root, Real-basis-function Method with Correct Branch-point Structure for Complex Resonances Energies. *Chem. Phys. Lett.* **1984**, *110*, 130-134.

17. McCurdy, C. W.; McNutt, J. F. On the Possibility of Analytically Continuing Stabilization Graphs to Determine Resonance Positions and Widths Accurately. *Chem. Phys. Lett.* **1983**, *94*, 306-310.

18. Mandelshtam, V. A.; Ravuri, T. R.; Taylor, H. S. Calculation of the Density of Resonance States Using the Stabilization Method. *Phys. Rev. Lett.* **1993**, *70*, 1932-1935.23.

19. Nooijen M.; Snijders, J. G. *J. Chem. Phys.* **1995**, *102*, 1681.

20. Stanton, J. F.; Gauss, J. Perturbative Treatment of the Similarity Transformed Hamiltonian in Equation-of-Motion Coupled-Cluster Approximations. *J. Chem. Phys.*, **1995**, *103*, 1064.

21. Dunning, T. H. Jr. Gaussian Basis Sets for Use in Correlated Molecular Calculations. I. The Atoms Boron through Neon and Hydrogen, *J. Chem. Phys.* **1989**, *90*, 1007-1023.
22. Kendall, R. A.; Dunning, T. H. Jr.; Harrison, R. J. Electron Affinities of the First-Row Atoms Revisited. Systematic Basis Sets and Wave Functions, *J. Chem. Phys.* **2002**, *96*, 6796-6806.
23. CFOUR, a quantum chemical program package written by Stanton, J.F.; Gauss, J.; Harding, M.E.; Szalay, P. G.; with contributions from Auer, A. A.; Bartlett, R. J.; Benedikt, U.; Berger, C.; Bernholdt, D. E.; Bomble, Y. J.; Cheng, L.; Christiansen, O.; Heckert, M.; Heun, O.; et al., and the integral packages MOLECULE (Almlöf, J; Taylor, P. R.), PROPS (Taylor, P. R.), ABACUS (Helgaker, T.; Jensen, Aa. H. J.; Jørgensen, P.; Olsen, J.), and ECP routines by Mitin, A. V. and van Wüllen C.
24. Landau, A.; Haritan, I. Kaprálová-Ždánská, P. R.; Moiseyev, N. Atomic and molecular complex resonances from real eigenvalues using standard (hermitian) electronic structure. calculations. *J. Phys. Chem. A* **2016**, *120*, 3098–3108.
25. Jordan, K. D. Construction of Potential Energy Curves in Avoided Crossing Situations. *Chem. Phys.* **1975**, *9*, 199-204.
26. Feshbach, H. A unified theory of nuclear reactions. II. Ann. Phys. (N.Y.) **1962**, *19*, 287.
27. S. Slimak, M. F. Falcetta, and K. D. Jordan, unpublished results.

